Available online at www.sciencedirect.com
SciVerse ScienceDirect
Ceramics International 39 (2013) 4105–4111
CERAMICS INTERNATIONAL
www.elsevier.com/locate/ceramint

Sol–gel mediated surface modification of nanocrystalline $NiFe_2O_4$ spinel powders with amorphous SiO_2

S. Vivekanandhan[a,d,e], M. Venkateswarlu[b], D. Carnahan[c], M. Misra[d,e], A.K. Mohanty[d,e], N. Satyanarayana[a,e,*]

[a]Department of Physics, Pondicherry University, Pondicherry 605014, India
[b]Research and Development, Amara Raja Batteries Ltd., Thirupathi 517520 Andhra Pradesh, India
[c]NanoLab Inc. Newton, MA 02458, USA
[d]School of Engineering, Thornbrough Building, University of Guelph, Guelph, ON, N1G 2W1, Canada
[e]Bioproducts Discovery and Development Centre, Department of Plant Agriculture, Crop Science Building, University of Guelph, Guelph, ON, N1G 2W1, Canada

Received 1 August 2012; received in revised form 27 September 2012; accepted 30 October 2012
Available online 6 November 2012

Abstract

Surface modification of nanocrystalline $NiFe_2O_4$ spinel particles with amorphous SiO_2 by the sol–gel process at 350 °C was demonstrated. Amorphous phase of the SiO_2 layer was evaluated by X-ray diffraction technique. Structural coordination of the pristine and SiO_2 coated $NiFe_2O_4$ particles as investigated by employing FTIR analysis. Thickness of the SiO_2 layer was investigated through transmission electron microscopy and it was identified to be ~10–23 nm over nanocrystalline $NiFe_2O_4$ particles. The magnetic behavior of pristine and surface modified $NiFe_2O_4$ particles were investigated using vibrating sample magnetometer (VSM). Magnetic studies showed the retention of magnetic property of surface modified $NiFe_2O_4$ particles with the reduced saturation magnetization and coercivity compared to the pristine $NiFe_2O_4$ particles, which is respectively due to the lower fraction of the magnetic component and the formation of interfacial structure.

Keywords: A. Sol–gel processes; B. Electron microscopy; C. Magnetic properties; D. Ferrites

1. Introduction

Nanocrystalline $NiFe_2O_4$ and their related materials have been were widely investigated for their unique magnetic properties including superparamagnetism and quantum tunneling of magnetization, which are significantly influenced by their size/shape and their combination with other materials [1–4]. These materials found applications in numerous fields including catalysis, sensor technology, electromagnetic shielding, water treatment, biomedical and biotechnology fields [5–10]. The common challenge in utilizing nanocrystalline magnetic materials including $NiFe_2O_4$ in various device applications is the retention of their physicochemical/magnetic properties, because of their strong tendency to aggregate and corrode due to the large surface reactivity [11]. In addition to that, the nanofabrication lowers the coordination between atoms in surface, which caused the reduction in magnetic moment compared to their respective bulk structures [12]. This can be addressed by introducing a coating structure on thesurfaces of magnetic particles, which suppresses the surface effect and also controls the inter-particle interactions. Guang-She et al. successfully demonstrated the reduction of this surface effect by dispersing nano-sized $NiFe_2O_4$ structures in a silica matrix [13].

Hence, surface modification of the magnetic materials receives great attention in the field of material research [14,15]. In addition to that, surface engineering of such magnetic materials creates additional functional properties that can be utilized for many diversified applications.

*Corresponding author at: Department of Physics, Pondicherry University, Pondicherry 605014, India. Tel.: +91 413 2654404; fax: +91 413 2655265.
E-mail address: nallanis2011@gmail.com (N. Satyanarayana).

0272-8842/$ - see front matter
http://dx.doi.org/10.1016/j.ceramint.2012.10.265

In general, shell structure has been made from either various kinds of polymers or silicates depend on the application requirements. Among them, silica is found to be an effective choice for the surface modification of magnetic core as a protective layer, which exhibits an enhanced corrosion resistance for the core materials, wide range of temperature operations, compatibility with bio-systems, non-toxicity, dielectric property, etc. [16]. Furthermore, the coating of SiO_2 layer over magnetic nanoparticles provides an effective encapsulation of the individual magnetic particles, which can prevent the interactions between the closely spaced magnetic particles. This will helps in inhibiting the nucleation and agglomeration of the magnetic particles during the additional processing [17]. As the demand for monodispersed magnetic materials increases surface modification of various types of magnetic materials received significant attention. Several groups have reported the fabrication and characterization of silica coated Fe_2O_3 [18,19], $CoFe_2O_4$ [20] and $NiFe_2O_4$ [21] nanomaterials. In addition to magnetic materials, SiO_2 coating was performed for various other metals [22,23], metal oxides [16,24] and metal chalcogenides [25,26] in literatures in order to improve their performance.

Fabrication process plays a key role in controlling the properties of SiO_2–magnetic materials interfaces and hence many processes were developed and explored. Sol–gel [4,27], poly-condensation procedure [28], microemulsion route [18], laser pyrolysis [29], etc., are a few common methods, which have been investigated for the surface modification of magnetic nano particles with SiO_2 layer. Among them, the sol– gel process is found to be a simple low temperature route, which has been extensively investigated for the uniform coating of SiO_2 layer on various types of nanostructure materials including magnetic particles with the better control of layer thickness [4,27]. However, very few reports are available for the sol–gel mediated synthesis of SiO_2:$NiFe_2O_4$ structures which are commonly called as composite materials, in which $NiFe_2O_4$ phase was dispersed in the SiO_2 matrix [4,13,30–33]. Recently, Larumbe et al. reported the auto-combustion method for the synthesis of SiO_2 coated $NiFe_2O_4$ using citric acid as fuel [21]. Their extensive microscopic study indicates the formation of $NiFe_2O_4$ phase in SiO_2 matrix. However, the surface modification/coating of $NiFe_2O_4$ particles with SiO_2 layer was not reported so far. Hence, in the present investigation, the surface modification of nanocrystalline $NiFe_2O_4$ particles with amorphous SiO_2 by the sol–gel process is reported. The surface modification process was investigated through TG/DTA, FTIR, XRD, SEM–EDS and TEM analysis. The magnetic properties of the pristine and SiO_2 coated nanocrystalline $NiFe_2O_4$ particles were identified through VSM studies.

2. Experimental

Nanocrystalline $NiFe_2O_4$ powders were prepared by polyacrylic acid and ethylene glycol assisted combustion route reported earlier [34]. Initially, 5 g of nanocrystalline $NiFe_2O_4$ powders was dispersed in acetone and sonicated for 30 min to remove agglomerations. Further, the particles were collected through centrifugation and the excess acetone was removed at 75 °C in hot air oven. 2 ml of TEOS was mixed with ethylalcohol by keeping them in equal volume under constant stirring. The obtained clear solution was mixed with water by keeping the TEOS and water mole ratio as 1:16, which is labeled solution A. Dried $NiFe_2O_4$ powders were dispersed in ethylalcohol and labeled as mixture B. Solutions A and B were mixed under constant stirring and the obtained sol was allowed to evaporate the excess water and alcohol. Further evaporation led to the formation of brown colored gel and the obtained gel was dried at 125 °C. Continuous drying resulted in the formation of dried mass; further it was calcined at 350 °C for the stabilization of SiO_2 shell on the surface of $NiFe_2O_4$ particles. Collected particles were used for further characterization. Schematic representation of the sol–gel process for the fabrication of SiO_2 coated nanocrystalline $NiFe_2O_4$ particles is shown in Fig. 1.

Thermal behavior of the evaporated gel coated $NiFe_2O_4$ particles were investigated using a TG/ DTA, Lybsys thermal analyzer, Setaram, France. Approximately 3 mg of SiO_2 xerogel coated $NiFe_2O_4$ particles was heated at the rate of 10 °C/ min from room temperature to 600 °C in flowing oxygen and the TG/ DTA thermograms were recorded . The Fourier-Transform Infrared Spectroscopy (FTIR) spectra were obtained employing Shimadzu FTIR - 8000 spectrometer. Synthesized specimens were mixed with KBr powder and the pressed pellets were examined between 400 and 4000 cm^{-1}. Scanning electron micrographs and elemental

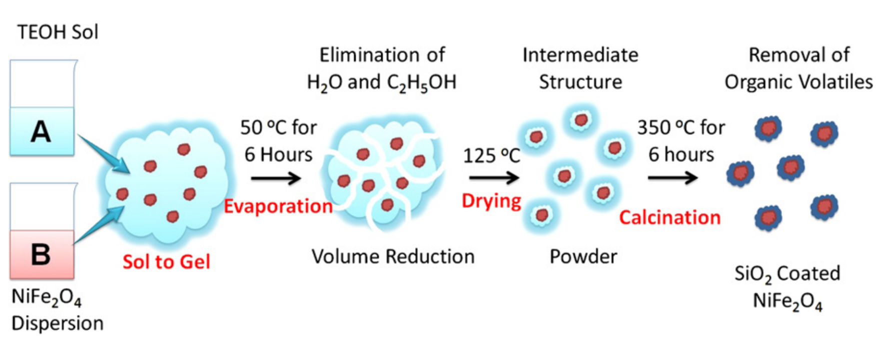

Fig. 1. Schematic representation of the solgel process for the surface modification of nanocrystalline $NiFe_2O_4$ powders with SiO_2.

mapping were taken using Hitachi, S-3400N, scanning electron microscope, Japan. Transmission electron microscopic (TEM) analysis of the SiO_2 coated $NiFe_2O_4$ nanoparticles were performed by JEOL-2010F transmission electron microscope, Japan with the accelerating voltage of 200 kV. The samples were deposited on carbon-coated copper grid from the dispersion made with high-purity acetone and the grid was dried prior to TEM analysis. X- ray diffraction patterns of the synthesized samples were recorded in X' Pert PRO MPD, PANalytical (Philips) X-ray powder diffractometer equipped with Cu K_a radiation. The average crystallite size of the $NiFe_2O_4$ powder was calculated through line broadening technique employing Scherrer's formula. Instrumental broadening was estimated using silicon standard obtained from national bureau of standards (NBS). Magnetic performance of the synthesized samples was investigated using a vibrating sample magnetometer (VSM), Lakeshore 7404.

3. Results and Discussions

3.1. TG/DTA analysis

Fig. 2 shows the TG/DTA thermogram of evaporated gel coated over $NiFe_2O_4$ particles recorded between 30 and 600 °C. The TG/DTA thermogram showed a major weight loss of about 75% observed between 50 and 150 °C which is due to the removal of excess water and ethanol, which are retained after the evaporation process in the gel coated on the surface of $NiFe_2O_4$ particles. This process absorbs energy and resulted in an endothermic peak in the same temperature region in the respective DTA curve. Further heating causes a gradual weight loss, which is identified at about 4% between 150 and 350 °C. This may be due to the removal of remaining organic volatiles from TEOS counterpart. However, there is no significant peak in DTA curve since the reaction would be mild. No more weight loss was observed above 350 °C, which indicates the complete removal of organic volatiles from the silica gel coated over the $NiFe_2O_4$ particles. Hence, 350 °C was optimized as the calcining temperature for the surface modification of nanocrystalline $NiFe_2O_4$ with SiO_2. From Fig. 2, the observed exothermic peak in DTA curve between 340 and 375 °C without any considerable weight loss indicates the formation of interfacial structure between $NiFe_2O_4$ core and SiO_2 shell,which is further it is supported by our VSM results.

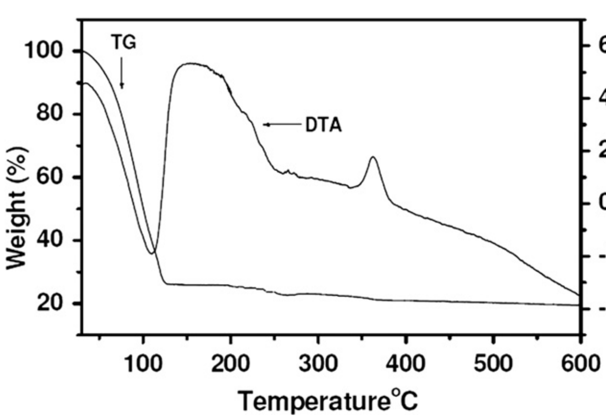

Fig. 2. TG/DTA thermogram of $NiFe_2O_4$ particles coated with dried gel (SiO_2 xerogel).

3.2. FTIR analysis

Structural coordination of the pristine and SiO_2 coated $NiFe_2O_4$ particles were investigated by FTIR analysis and

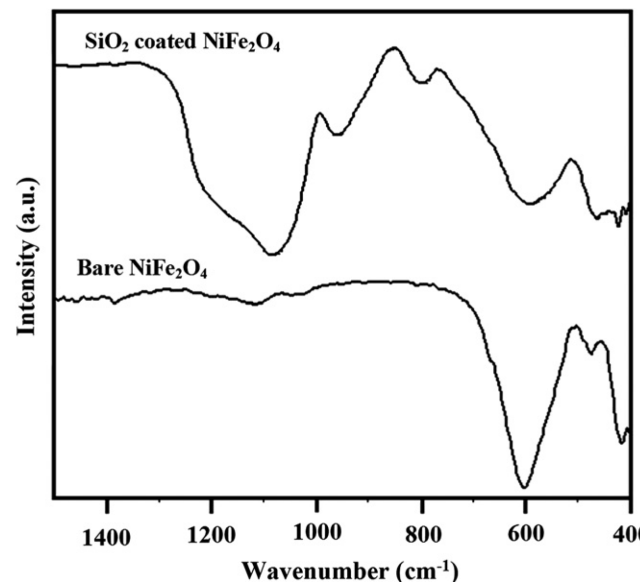

Fig. 3. FTIR spectra of pristine and silica (SiO_2) coated nanocrystalline $NiFe_2O_4$ powders.

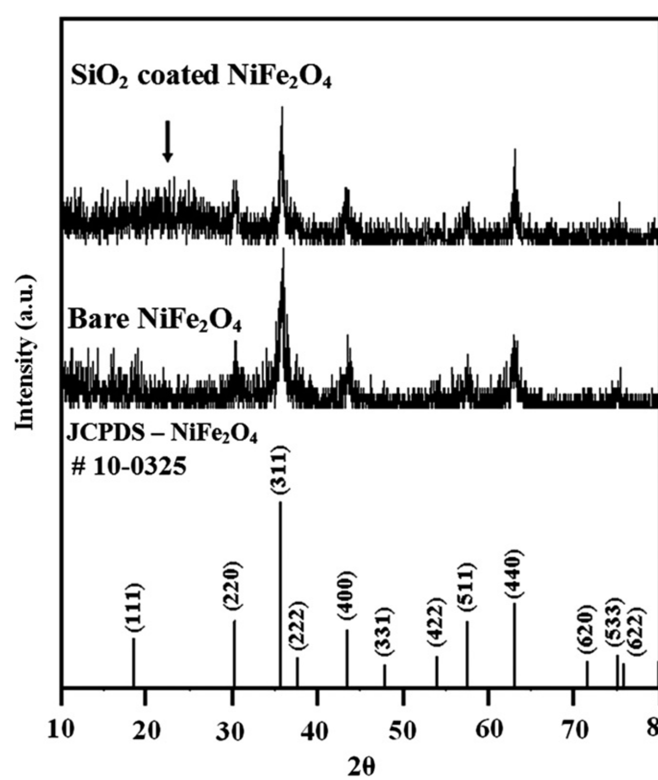

Fig. 4. XRD patterns of pristine and silica coated nanocrystalline $NiFe_2O_4$ powders.

the recorded spectra are shown in Fig. 3. The FTIR spectra reveal the coordinated position of the metal ions and their vibration modes, which provides the clear information of their structural features of the pristine and SiO_2 coated nanocrystalline $NiFe_2O_4$ particles. From Fig. 3, the FTIR spectrum of pristine $NiFe_2O_4$ shows two peaks at 604 cm^{-1} and 412 cm^{-1} and these are attributed to the tetrahedral and octahedral complexes of $Fe_2O_4^{2-}$ group respectively, which confirmed the $NiFe_2O_4$ structure [35]. The observed difference in the peak values is due to the variation in ionic distance between $Fe^{3+}$and O^{2-} in their octahedral and tetrahedral counterparts. From Fig. 3, the FTIR spectra of SiO_2 coated $NiFe_2O_4$ powder exhibit high intense absorption peaks at 1200 cm^{-1} and 1089 cm^{-1} and these peaks are assigned to the longitudinal and transverse stretching vibration modes of the Si–O–Si asymmetric bond respectively. Additional bands at 800 cm^{-1} and 460 cm^{-1} are also indentified as the characteristic peaks of Si–O–Si bond respectively. The other peak observed at 960 cm^{-1} assigned to the SiO_3^{-2} vibrations indicates the existence of nonbridging oxygen ions [36]. In addition to that, the peaks attributed to metal–O–Si bonds are also reported in the same frequency range, which supports the possible formation of Fe–O–Si interfacial structure [36]. The observed peaks, which are assigned to SiO_2 structure ensure the formation of SiO_2 layer over $NiFe_2O_4$ particles; further it was confirmed by SEM- EDS elemental mapping and TEM analysis as follows.

3.3. XRD analysis

Fig. 4 shows the XRD patterns of pristine and surface modified $NiFe_2O_4$ nanostructures alongwith JCPDS standard. From Fig. 4, the observed XRD pattern for the pristine $NiFe_2O_4$ powders prepared by polymeric precursor route at 450 °C shows major high intense characteristic peaks at 30, 36, 43 and 63 2θ values which are assigned to (2 2 0), (3 1 1), (4 0 0) and (4 4 0) planes respectively. These obtained peaks

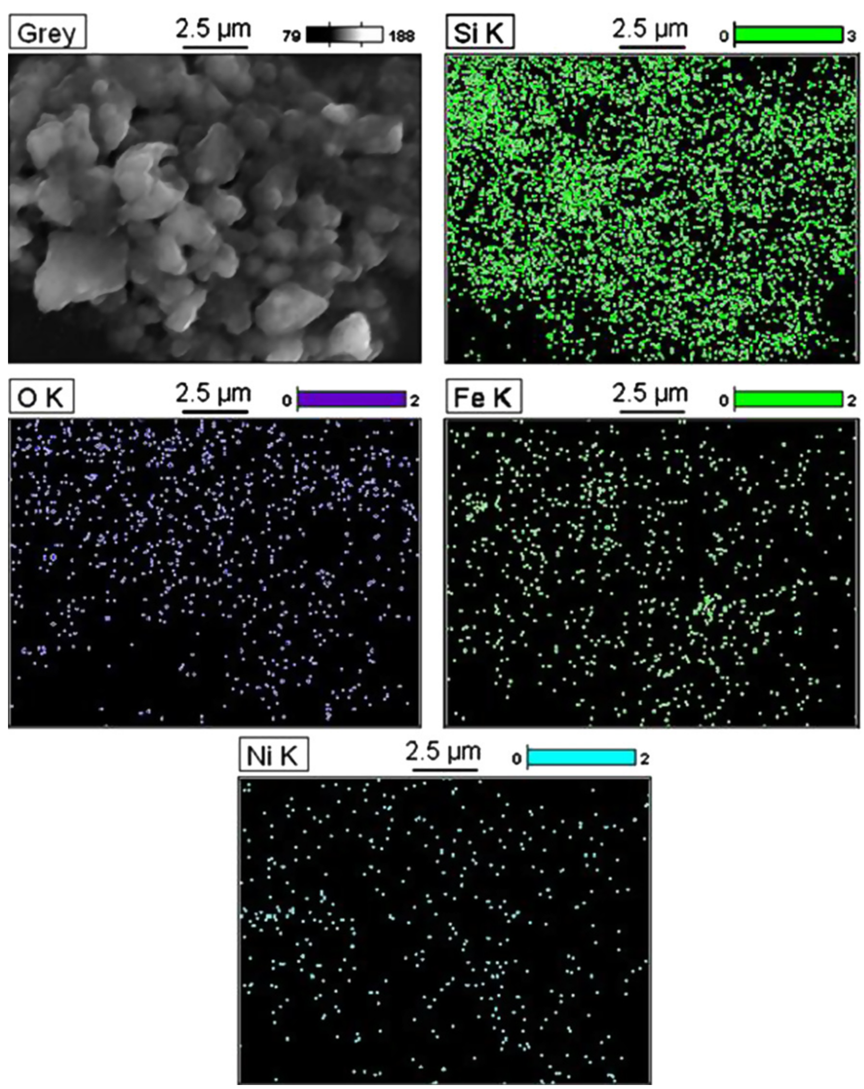

Fig. 5. SEM-EDS elemental mappings of nanocrystalline $NiFe_2O_4$ powders coated with SiO_2.

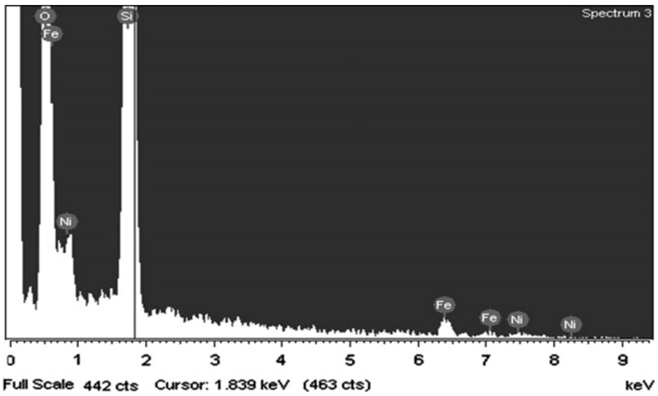

Fig. 6. SEM-EDS spectrum of nanocrystalline $NiFe_2O_4$ powders coated with SiO_2.

Table 1
SEM-EDS analysis results of SiO_2 coated nanocrystalline $NiFe_2O_4$ particles.

Element	App conc.	Intensity corrn.	Wt%	At%
O K	11.29	1.4552	39.84	60.05
Si K	6.38	0.9818	33.33	28.62
Fe L	1.14	0.4126	14.22	6.14
Ni L	1.02	0.4162	12.61	5.18
Totals			**100.00**	**100.00**

were well consistent with the JCPS standard values, which confirms the formation of phase pure cubic $NiFe_2O_4$ particles. The crystallite size of pristine $NiFe_2O_4$ powders was calculated for all possible intense reflections using Scherrer's formula and the average crystallite size was found to be ~15.3 nm. The XRD pattern of SiO_2 coated $NiFe_2O_4$ powder exhibits a new broad peak at 22° along with the characteristic peaks of the $NiFe_2O_4$ phase, which confirms the existence of SiO_2 structure. occurrence of broad peak corresponding to SiO_2 structure of clearly indicates the formation of amorphous SiO_2 layer on the nanocrystalline $NiFe_2O_4$ powder. The average crystallite size of SiO_2 coated $NiFe_2O_4$ powder was found to be ~15.1 nm. This indicates that the sol gel process for the surface coating of $NiFe_2O_4$ particles does not change its crystallite size. Further, the lattice parameter was calculated for both pristine and SiO_2 coated $NiFe_2O_4$ powders and they are respectively found to be $a=8.3554$ Å and 8.3631 Å, which are very much comparable with the values reported in the literatures [37,38]. The observed invariant in the calculated lattice parameters ensured that the $NiFe_2O_4$ powders, coated with SiO_2, maintained its original structure and symmetry.

3.4. SEM– EDS elemental mapping analysis

The scanning electron micrograph of surface modified nanocrystalline $NiFe_2O_4$ particles with SiO_2 along with the

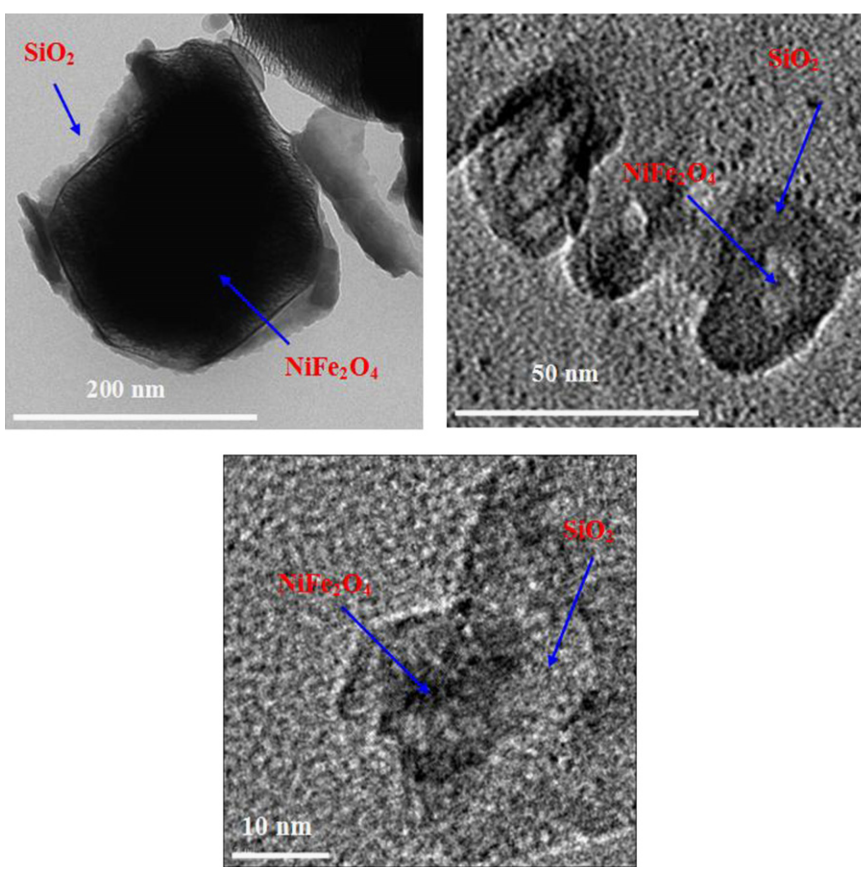

Fig. 7. TEM micrographs of nanocrystalline $NiFe_2O_4$ powders coated with SiO_2 with different magnifications.

elemental mapping using energy dispersive spectroscopy (EDS) is shown in Fig. 5. The SEM micrograph of $NiFe_2O_4$ particles coated with amorphous SiO_2 layer shows agglomeration. Respective EDS spectrum and elemental mappings of SiO_2 coated $NiFe_2O_4$ particles indicate the presence and the uniform distribution of Si along with Fe and Ni, which confirm the coating of SiO_2 structure on $NiFe_2O_4$ particle surface. SEM- EDS spectrum of the $NiFe_2O_4$ particles coated with SiO_2 is shown in Fig. 6. Also, the observed elemental informations from SEM-EDS analysis are given in Table 1, which confirms the presence of Si with the composition of 33.33 wt%.

3.5. TEM analysis

TEM image of the surface modified nanocrystalline $NiFe_2O_4$ particles with SiO_2 is shown in Fig. 7. From Fig. 7, the observed particle size for the core $NiFe_2O_4$ is about 10–20 nm and these values are in consistence with the average crystallite size obtained from the XRD analysis. Higher particle size, observed in TEM analysis, clearly indicates the poly-crystallinity of the $NiFe_2O_4$ particles. In addition to that, TEM images clearly indicate the formation of thin SiO_2 layer on core $NiFe_2O_4$ particles with the size of 10–23 nm. The coating thickness varies from particle to particle, which can be controlled by optimizing the evaporation and drying process. The observed two different distinguished layers observed in TEM micrograph confirmed the formation of SiO_2 layer on $NiFe_2O_4$ particles.

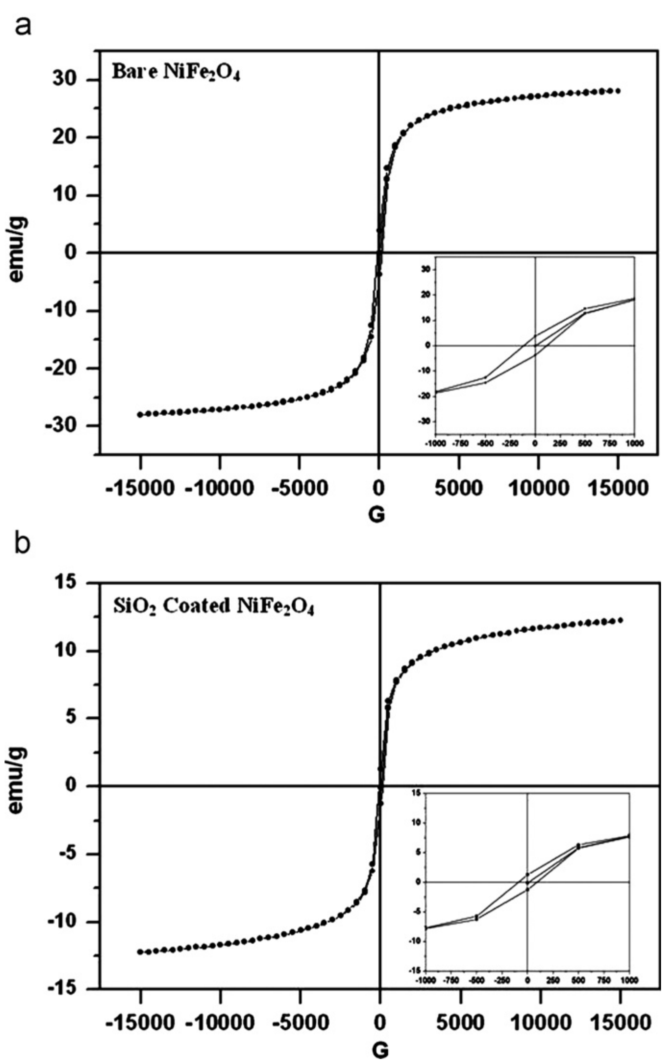

Fig. 8. Magnetization curve of the pristine (a) and SiO_2 coated (b) nanocrystalline $NiFe_2O_4$ powders.

3.6. Magnetic properties through VSM

Field dependent magnetization plots (M–H curve) of the pristine and surface modified nanocrystalline $NiFe_2O_4$ powders are shown in Fig. 8. The M–H curve of the pristine nanocrystalline $NiFe_2O_4$ particles showed the magnetic behavior with the higher magnetization value (saturation magnetization (M_s) 28.039 emu/g) than the M_s values of SiO_2 coated $NiFe_2O_4$ powders (12.247 emu/g). The decreased M_s value is not only attributed to the lower density of the magnetic component in the SiO_2 coated $NiFe_2O_4$ powders but also due to the higher surface disorder and a spin-glass configuration at the contact region between the silica shell and the $NiFe_2O_4$ nanoparticles [21]. Also, the observed significant decrease in the coercivity of SiO_2 coated $NiFe_2O_4$ powders (90.33 G) compared to the pristine $NiFe_2O_4$ powders (114.91 G) is due to the formation of interfacial structure. Yi et al. reported a similar magnetic behavior for the SiO_2/Fe_2O_3 nano-architectures [15]. SiO_2 shell thickness and the formation of interfacial structures can be controlled precisely by altering various synthesis parameters of the sol–gel process.

4. Conclusions

The solgel process was successfully employed for the surface modification of nanocrystalline $NiFe_2O_4$ powders with amorphous SiO_2 layer. XRD, FTIR, SEM-EDS and TEM analyses confirmed the formation of SiO_2 layer over $NiFe_2O_4$ particles. From XRD analysis, it is confirmed that the coated SiO_2 layer was in the amorphous phase. VSM analysis confirms the magnetic behavior for both pristine and SiO_2 coated nanocrystalline $NiFe_2O_4$ powders. However, coating of amorphous SiO_2 layer reduced the saturation magnetization and coercivity, which are respectively due to the lower content of the magnetic component (due to the SiO_2 coating) and the formation of interfacial structure.

Acknowledgements

Dr. N. Satyanarayana gratefully acknowledges DST, CSIR, DRDO, Government of India, for the financial support through major research projects. SV acknowledges the CSIR, Government of India, for the award of Senior Research Fellowship.

References

[1] N. Ponpandian, P. Balaya, A. Narayanasamy, Electrical conductivity and dielectric behaviour of nanocrystalline $NiFe_2O_4$ spinel, Journal of Physics: Condensed Matter 14 (12) (2002) 3221.

[2] H. Zhao, X. Sun, C. Mao, J. Du, Preparation and microwave-absorbing properties of $NiFe_2O_4$–polystyrene composites, Physica B: Condensed Matter 404 (1) (2009) 69–72.

[3] Y. Liu, L. Gao, A study of the electrical properties of carbon nanotube–NiFe $_2O_4$ composites: effect of the surface treatment of the carbon nanotubes, Carbon 43 (1) (2005) 47–52.

[4] L. Li, G. Li, R. Smith Jr, H. Inomata, Microstructural evolution and magnetic properties of $NiFe_2O_4$ nanocrystals dispersed in amorphous silica, Chemistry of Materials 12 (12) (2000) 3705–3714.

[5] K. Gavrilenko, T. Mironyuk, V. Il'in, S. Orlik, V. Pavlishchuk, From heteronuclear complex to composite oxide approach in the synthesis of nanosized ferrites $M^{II}Fe_2^{III}O\ _4$ (M=Mn, Co, Ni) with spinel structure and their catalytic properties, Theoretical and Experimental Chemistry 38 (2) (2002) 118–124.

[6] Y.L. Liu, H. Wang, Y. Yang, Z.M. Liu, H.F. Yang, G.L. Shen, R.Q. Yu, Hydrogen sulfide sensing properties of $NiFe_2O_4$ nanopowder doped with noble metals, Sensors and Actuators, B: Chemical 102 (1) (2004) 148–154.

[7] A. Tomitaka, H. Kobayashi, T. Yamada, M. Jeun, S. Bae, Y. Takemura, Magnetization and self-heating temperature of $NiFe_2O_4$ nanoparticles measured by applying ac magnetic field, Journal of Physics: Conference Series 200 (2010) 122010–122016.

[8] S.W. Lee, S. Bae, Y. Takemura, E. Yamashita, J. Kunisaki, S. Zurn, C.S. Kim, Magnetic properties, self-temperature rising characteristics, and biocompatibility of $NiFe_2O_4$ nanoparticles for hyperthermia applications, IEEE Transactions on Magnetics 42 (10) (2006) 2833–2835.

[9] M. Phadatare, V. Khot, A. Salunkhe, N. Thorat, S. Pawar, Studies on polyethylene glycol coating on $NiFe_2O_4$ nanoparticles for biomedical applications, Journal of Magnetism and Magnetic Materials 324 (2012) 770–772.

[10] Y. Köseoğlu, Superparamagnetic $NiFe_2O_4$ nanoparticles to remove arsenic from drinking water, in: Proceedings of the 2nd International Symposium on Sustainable Development, Sarajevo, June 8–9, 2010.

[11] H. Srikanth, R. Hajndl, C. Chirinos, J. Sanders, A. Sampath, T. Sudarshan, Magnetic studies of polymer-coated Fe nanoparticles synthesized by microwave plasma polymerization, Applied Physics Letters 79 (2001) 3503.

[12] R. Kodama, Magnetic nanoparticles, Journal of Magnetism and Magnetic Materials 200 (1) (1999) 359–372.

[13] L. Guang-She, L. Li-Ping, R. Smith, H. Inomata, Characterization of the dispersion process for $NiFe_2O_4$ nanocrystals in a silica matrix with infrared spectroscopy and electron paramagnetic resonance, Journal of Molecular Structure 560 (1) (2001) 87–93.

[14] A.K. Gupta, M. Gupta, Synthesis and surface engineering of iron oxide nanoparticles for biomedical applications, Biomaterials 26 (18) (2005) 3995–4021.

[15] D.K. Yi, S.S. Lee, G.C. Papaefthymiou, J.Y. Ying, Nanoparticle architectures templated by SiO_2/Fe_2O_3 nanocomposites, Chemistry of Materials 18 (3) (2006) 614–619.

[16] H. Cui, G. Hong, X. Wu, Y. Hong, Silicon dioxide coating of CeO_2 nanoparticles by solid state reaction at room temperature, Materials Research Bulletin 37 (13) (2002) 2155–2163.

[17] H. Wang, W. Zhang, F. Zhang, Y. Cao, W. Su, The effect of 3-aminopropyltrimethoxysilane on the formation of $NiFe_2O_4/SiO_2$ nanocomposites, Journal of Magnetism and Magnetic Materials 320 (13) (2008) 1916–1920.

[18] T. Tago, T. Hatsuta, K. Miyajima, M. Kishida, S. Tashiro, K. Wakabayashi, Novel synthesis of silicacoated ferrite nanoparticles prepared using waterinoil microemulsion, Journal of the American Ceramic Society 85 (9) (2002) 2188–2194.

[19] A.P. Philipse, M.P.B. Van Bruggen, C. Pathmamanoharan, Magnetic silica dispersions: preparation and stability of surface-modified silica particles with a magnetic core, Langmuir 10 (1) (1994) 92–99.

[20] L. Zhao, H. Yang, Y. Cui, X. Zhao, S. Feng, Study of preparation and magnetic properties of silica-coated cobalt ferrite nanocomposites, Journal of Materials Science 42 (11) (2007) 4110–4114.

[21] S. Larumbe, J. Pe′ rez-Landaza′ bal, J. Pastor, C. Go′ mez-Polo, Sol-gel $NiFe_2O_4$ nanoparticles: Effect of the silica coating, Journal of Applied Physics 111 (10) (2012) 103911–103918.

[22] M. Kishida, T. Tago, T. Hatsuta, K. Wakabayashi, Preparation of silica-coated rhodium nanoparticles using water-in-oil microemulsion, Chemistry Letters 29 (9) (2000) 1108–1109.

[23] T. Tago, Y. Shibata, T. Hatsuta, K. Miyajima, M. Kishida, S. Tashiro, K. Wakabayashi, Synthesis of silica-coated rhodium nanoparticles in reversed micellar solution, Journal of Materials Science 37 (5) (2002) 977–982.

[24] Y. Liu, C. Ge, M. Ren, H. Yin, A. Wang, D. Zhang, C. Liu, J. Chen, H. Feng, H. Yao, Effects of coating parameters on the morphology of SiO_2-coated TiO_2 and the pigmentary properties, Applied Surface ScienceAppl. Surf. Sci. 254 (9) (2008) 2809–2819.

[25] O.C. Monteiro, A.C.C. Esteves, T. Trindade, The synthesis of SiO_2@ CdS nanocomposites using single-molecule precursors, Chemistry of Materials 14 (7) (2002) 2900–2904.

[26] Y. Wang, Z. Tang, X. Liang, L.M. Liz-Marzán, N.A. Kotov, SiO_2-coated CdTe nanowires: bristled nano centipedes, Nano Letters 4 (2) (2004) 225–231.

[27] T. Tago, S. Tashiro, Y. Hashimoto, K. Wakabayashi, M. Kishida, Synthesis and optical properties of SiO_2-coated CeO_2 nanoparticles, Journal of Nanoparticle Research 5 (1) (2003) 55–60.

[28] N.D.S. Mohallem, L.M. Seara, Magnetic nanocomposite thin films of $NiFe_2O_4/SiO_2$ prepared by sol–gel process, Applied Surface Science 214 (1-4) (2003) 143–150.

[29] O. Bomatí-Miguel, Y. Leconte, M. Morales, N. Herlin-Boime, S. Veintemillas-Verdaguer, Laser pyrolysis preparation of SiO_2-coated magnetic nanoparticles for biomedical applications, Journal of Magnetism and Magnetic Materials 290 (2005) 272–275.

[30] S.M. Montemayor, L. Garcia-Cerda, J. Torres-Lubian, O. Rodriguez-Fernandez, Comparative study of the synthesis of $CoFe_2O_4$ and $NiFe_2O_4$ in silica through the polymerized complex route of the sol–gel method, Journal of Sol–Gel Science and Technology 42 (2) (2007) 181–186.

[31] H. Wang, F. Zhang, W. Zhang, X. Wang, Z. Lu, Z. Qian, Y. Sui, D. Dong, W. Su, The effect of surface modification on the morphology and magnetic properties of $NiFe_2O_4$ nanoparticles, Journal of Crystal Growth 293 (1) (2006) 169–174.

[32] X.M. Liu, S.Y. Fu, C.J. Huang, Magnetic properties of Ni ferrite nanocrystals dispersed in the silica matrix by sol–gel technique, Journal of Magnetism and Magnetic Materials 281 (2) (2004) 234–239.

[33] A. Hutlova, D. Niznansky, J. Plocek, J. Bursik, J.L. Rehspringer, Nanocomposites $NiFe_2O_4/SiO_2$ and $CoFe_2O_4/SiO_2$–preparation by Sol-Gel method and physical properties, Journal of Sol–Gel Science and Technology 26 (1) (2003) 473–477.

[34] S. Vivekanandhan, M. Venkateswarlu, N. Satyanarayana, Effect of ethylene glycol on polyacrylic acid based combustion process for the synthesis of nano-crystalline nickel ferrite ($NiFe_2O_4$), Materials Letters 58 (22) (2004) 2717–2720.

[35] M. Gotic, I. Czako-Nagy, S. Popovic, S. Music, Formation of nanocrystalline $NiFe_2O_4$, Philosophical Magazine Letters 78 (3) (1998) 193–201.

[36] F. Monte, W. Larsen, J.D. Mackenzie, Stabilization of tetragonal ZrO_2 in ZrO_2–SiO_2 binary oxides, Journal of the American Ceramic Society 83 (3) (2004) 628–634.

[37] H. Perron, T. Mellier, C. Domain, J. Roques, E. Simoni, R. Drot, H. Catalette, Structural investigation and electronic properties of the nickel ferrite $NiFe_2O_4$: a periodic density functional theory approach, Journal of Physics: Condensed matter 19 (34) (2007) 346219.

[38] S.H. Lee, S.J. Yoon, G.J. Lee, H.S. Kim, C.H. Yo, K. Ahn, D.H. Lee, K.H. Kim, Electrical and magnetic properties of $NiCr_x$-$Fe_{2-x}O_4$ spinel (0 ≤ <i> x </i> ≤ 0.6), Materials Chemistry and Physics 61 (2) (1999) 147–152.